Petroleum Science 22 (2025) 5203–5211

Contents lists available at ScienceDirect

Petroleum Science

journal homepage: www.keaipublishing.com/en/journals/petroleum-science

Original Paper

Swelling kinetics of polymer microspheres used for conformance control and their matching mechanisms with oil reservoir fractures

Hong-Bin Yang [a,b,c,*], Lu-Yao Xing [a,b,c], Ting-Feng Liu [d], Miao Li [e], Jie Geng [a,b,c], Yang Zhang [d], Yu-Bin Zhang [a,b,c], Rui-Chao Wang [a,b,c], Bauyrzhan Sarsenbekuly [f], Wan-Li Kang [c], Li-Ming Zhang [g]

[a] State Key Laboratory of Deep Oil and Gas, China University of Petroleum (East China), Qingdao, 266580, Shandong, PR China
[b] Shandong Key Laboratory of Oil and Gas Field Chemistry, Qingdao, 266580, Shandong, PR China
[c] School of Petroleum Engineering, China University of Petroleum (East China), Qingdao, 266580, Shandong, PR China
[d] Petroleum Engineering Technology Research Institute, Shengli Oilfield Branch of Sinopec, Dongying, 257000, Shandong, PR China
[e] Qingdao Huizhi Oilfield Service Company Limited, Qingdao, 266580, Shandong, PR China
[f] Kazakh-British Technical University, Almaty 050000, Kazakhstan
[g] School of Petroleum Engineering and Environmental Engineering, Yan'an University, Yan'an, 716000, Shaanxi, PR China

ARTICLE INFO

Article history:
Received 22 April 2025
Received in revised form
3 November 2025
Accepted 4 November 2025
Available online 12 November 2025

Edited by Yan-Hua Sun

Keywords:
Polymer microspheres
Elastic modulus
Swelling kinetics
Matching mechanism

ABSTRACT

Polymer microspheres are one type of particle gel with swelling property, and the particle size is distributed between nanometer and micron. Because of the good variability and migration characteristics, polymer microspheres are widely used as conformance control agents, especially in fractured reservoirs. However, in the application process, the matching between polymer microspheres and the size of reservoir fractures remains insufficiently studied, leading to prevalent blind applications and low utilization efficiency. Based on polymer microspheres with different elastic modulus (23.6–715 Pa) prepared in the laboratory, the swelling dynamics of polymer microspheres were established according to their swelling ratio data under different reservoir temperatures (20–80 °C). The fracture plate model was used to simulate the fractured reservoir, the matching mechanism of polymer microspheres in the model was studied. Applying this model and equation $p_t = kG' + m$, we further investigated the quantitative relationship between threshold pressure and elastic modulus of polymer microspheres in the fracture plate model in the migration process. The swelling ratio of polymer microspheres showed that the polymer microspheres absorbed water quickly in the early stage and gradually slowed down in the later stage. The characteristics of the early stage were simulated by Fickian equation and those of the later stage were simulated by Schott equation. A new swelling kinetic equation of polymer microspheres was established considering the whole swelling characteristics. The diameter/width ratio was used as an evaluation index, the matching property results showed that under the experimental conditions, the migration modes of microspheres in the fracture plate model were straight-through passage, deformable passage, and blockage. Under the same elastic modulus, the smaller the fracture aperture, the higher the threshold pressure. At the same fracture aperture, the threshold pressure increased with the increase in elastic modulus. Based on the obtained results, the value range of threshold pressure under different fracture apertures could be quantitatively predicted, and then the particle size and elastic modulus of the polymer microspheres for conformance control could be determined according to the reservoir fracture parameters. The blind use of polymer microspheres for conformance control agents should be avoided, the success rate of fractured reservoir of conformance control could be improved. The results of the study have experimental guidance for the conformance control scheme design of polymer microspheres.

* Corresponding author.
E-mail address: hongbinyang@upc.edu.cn (H.-B. Yang).

Peer review under the responsibility of China University of Petroleum (Beijing).

https://doi.org/10.1016/j.petsci.2025.11.011

1. Introduction

With the advancement of oil and gas exploration in complex formations, water channeling through high-permeability zones remains a critical recovery challenge. Conventional plugging agents suffer from inherent limitations: (1) Their poor deformability results in insufficient adaptation to fracture structures (Shagymgereyeva et al., 2023; Wang et al., 2019). (2) They often suffer from thermal instability, leading to premature degradation under high-temperature conditions in deep reservoirs. In contrast, swellable polymer microspheres address these shortcomings through tunable elasticity and thermoresponsive swelling (Cao M. J. et al., 2021; Jie et al., 2024; Lu et al., 2023; Zhao et al., 2016). Among them, polymer microspheres show great application potential in the field of conformance control because of their unique water swelling property and good plugging effect (Li et al., 2020; Zhao et al., 2020). Polymer microspheres (Yang et al., 2025b) control formation water flow by adjusting their swelling properties, thereby optimizing water injection conformance, improving sweep efficiency, and ultimately enhancing oil recovery (Dai et al., 2023; Yang et al., 2024). Despite the success of polymer microspheres in field applications, the underlying interaction mechanism with reservoir fractures is not fully elucidated. This knowledge gap hinders the optimization of their application effectiveness (Liu et al., 2024). The aperture, shape, and distribution characteristics of fractures in the reservoir are complex and diverse, which have a significant impact on the migration and plugging effect of polymer microspheres (Liu et al., 2020; Wu et al., 2021). If polymer microsphere size and elastic modulus are incompatible with fracture characteristics, the microspheres may fail to be injected into fractures effectively or may become trapped and rupture within them. This compromises plugging effectiveness and sweep efficiency enhancement (Li et al., 2019; Song et al., 2023).

In view of the matching mechanism of polymer microspheres and reservoir fractures, many scholars have carried out a lot of innovative work (Wang et al., 2022; Yang et al., 2017). Chen et al. (2020) demonstrated through dual-scale experiments that microspheres with higher swelling ratios preferentially achieve deep migration via deformation, exhibiting superior direct-blockage strength over smaller microspheres' bridging mechanisms. Zhao and Pu (2020) identified a critical elasticity modulus threshold, showing that microspheres with matching coefficients > 1.2 and modulus exceeding 10 kPa enhance resistance coefficients by > 70% and achieve > 96% plugging efficiency through shear deformation resistance. Yang et al. (2025c) revealed via fluorescence experiments that high-elasticity microspheres improve sweep efficiency by through “piston-like” migration, compared with low-elasticity polymer microspheres.

In terms of water swelling kinetics, the researchers deeply analyzed the water swelling process of polymer microspheres and its influencing factors by establishing theoretical models and carrying out experimental measurements (Wang et al., 2014; Yan et al., 2024). Researchers established multi-physics models considering temperature, ionic strength, and crosslinking density. Advanced characterization techniques, including in situ dynamic light scattering (DLS) and synchrotron X-ray microscopy, were deployed to track real-time diameter changes (Cheng et al., 2024; Hou et al., 2020; Li et al., 2024). These studies reveal the basic laws and characteristics of water swelling of polymer microspheres, and provide a theoretical basis for optimizing the performance of microspheres and improving the plugging effect (Jiang et al., 2025; Yang et al., 2026). While foundational swelling models exist for polymer gels, notably the time-temperature superposition approach achieving $R^2 = 0.89$ for bulk hydrogels (Yang et al., 2025a). The existing models for the swelling kinetics of microspheres do not comprehensively take into account the different stages of water absorption and swelling of the microspheres. As a result, the experimental results in the initial and later stages of swelling have significant discrepancies (Hua et al., 2014; Zhong et al., 2018). Based on the swelling behavior of polymer microspheres, we developed a dynamic swelling equation and theoretical framework through rigorous fitting of experimental data. On the basis of considering the elastic modulus of polymer microspheres, the matching mechanism of polymer microspheres and reservoir fractures was discussed in depth. In the process of research, the fracture plate model was used to simulate the experiment. By varying parameters like fracture aperture and elastic modulus, we systematically documented microsphere transport patterns under diverse conditions and established the quantitative relationship between polymer microsphere threshold pressure and elastic modulus. Through these studies, it is expected to deeply reveal the matching mechanism between polymer microspheres and reservoir fractures, and provide scientific basis and technical support for understanding the mechanism of improving oil recovery.

2. Experimental materials and methods

2.1. Materials

The relative molecular weight of partially hydrolyzed polyacrylamide (HPAM) is 2700×10^4 Da, with a degree of hydrolysis of 23.8%. It is an industrial product. The information of the polymer microspheres used is shown in Table 1. LEM-1 is a polymer microsphere formed by inverse suspension polymerization, with an initial particle size of 100.6 μm and an elastic modulus of 23.6 Pa (Yang et al., 2018; Tao et al., 2016). LEM-2, HEM-1, HEM-2, and HEM-3 are polymer microspheres developed in the laboratory synthesis using the same method. The difference lies in the amount of crosslinking agent added during the polymerization process, which results in different elastic modulus for the obtained polymer microspheres. They are named LEM-2, HEM-1, HEM-2, and HEM-3 according to the magnitude of their elastic modulus. Sodium chloride, potassium chloride, calcium chloride, magnesium chloride hexahydrate, sodium sulfate, anhydrous sodium carbonate, sodium bicarbonate, are analytically pure, produced by State Pharmaceutical Group Chemical Reagents Co., Ltd. The ion composition of simulated formation water is shown in Table 2.

2.2. Methods

2.2.1. Swelling property measurement

The swelling property of polymer microspheres was measured by weighing method (Yang et al., 2020). The pre-weighed nylon mesh filter bag with dry microspheres sample was completely immersed in simulated water at a certain temperature. After a certain period of time, the filter bag was taken out, and the excess water on the surface of the microspheres was wiped off with filter paper. The swelling ratio can be expressed as

Table 1
Elastic modulus of polymer microspheres used in this work.

Type of polymer microsphere	Source	G', Pa
LEM-1	Laboratory synthesis	23.6
LEM-2	Laboratory synthesis	32.5
HEM-1	Laboratory synthesis	121
HEM-2	Laboratory synthesis	466
HEM-3	Laboratory synthesis	715

$$S_r = \frac{m_t - m_0}{m_0} \quad (1)$$

where S_r is the swelling ratio, g/g; m_0 is the dry weight of polymer microspheres, g; m_t is the wet weight of polymer microspheres after swelling for a certain time, g.

2.2.2. Microstructure measurement

The particle size of polymer microspheres was observed by an XSJ-2 optical microscope (Chongqing photoelectric, China). Samples were prepared by dispersing microspheres in deionized water via ultrasonic treatment (40 kHz, 5 min), followed by deposition on pre-cleaned glass slides (Cao B. et al., 2021a; Jiang et al., 2024). Each sample was analyzed using the integrated image processing software, and the dimension measurement was calculated according to the standard.

2.2.3. Compatibility evaluation method of microspheres and fractures

The fracture plate model developed in the laboratory is used to simulate the large fracture in the reservoir, and the aperture of the fracture is determined by the width of the gasket between the two glass plates (Barros-Galvis et al., 2018). Fig. 1 is the picture and schematic diagram of fracture plate model, in which the size of the upper and lower glass plates is 24 cm × 24 cm × 2 cm. According to the change of injection pressure and microsphere particle size, the matching relationship between microsphere performance and fracture size is established (Diwu et al., 2018; Du et al., 2020). Fig. 2 is the flow chart of the fracture plate model displacement experiment. The specific process is as follows:

(1) A certain concentration of polymer microsphere conformance control system (1000 mg/L polymer microsphere + 1000 mg/L HPAM) was prepared. After stirring and dispersing evenly, it was placed in a thermostat at 50 °C for 48 h to make it fully swollen.
(2) After the fracture plate model was saturated with simulated formation water, the swollen conformance control system was added to the accumulator, and the magnetic stirrer at the lower part of the accumulator was started to ensure the good dispersion of the conformance control system, and then the experimental device was connected according to the experimental flow chart of Fig. 2.
(3) The polymer microsphere conformance control system was injected into the model at an injection rate of 3 mL/min, and the injection pressure at different time intervals was recorded. At the same time, the morphology of the microspheres in the output liquid at the outlet end were observed and measured by the optical microscope, and compared with the morphology of the microspheres before injection.
(4) According to the change of pressure during microsphere injection and the change of microsphere particle size at the outlet end, the matching relationship between microsphere performance and fracture parameters was established.

3. Results and discussion

3.1. Swelling kinetics equation and theoretical chart of low elastic polymer microspheres

Fig. 3 shows the swelling curve of LEM-1 in DG oilfield formation water at different temperatures. It can be seen from Fig. 3 that the swelling process of LEM-1 basically goes through two stages at different temperatures. At the same temperature, with the increase in swelling time, the swelling ratio initially increases and then tends to level off. The higher the temperature, the greater the final swelling ratio. By analyzing and fitting the swelling ratio during the swelling process, the swelling kinetic equation that can completely describe the swelling process of LEM is finally proposed.

3.1.1. Initial swelling process–Fickian equation

During initial swelling, water molecules permeate and diffuse within low-modulus polymer microspheres, driving a dual-mechanism swelling process characterized by Fickian and non-Fickian behavior (Budianto and Amalia, 2020). The swelling ratio S_{rt} of the low elastic polymer microspheres is exponentially related to the swelling time t. The swelling kinetic equation is as follows:

Table 2
The ion composition of simulated formation water.

Ion content, mg/L							Total salinity, mg/L
$K^+ + Na^+$	Mg^{2+}	Ca^{2+}	Cl^-	SO_4^{2-}	HCO_3^-	CO_3^{2-}	
2043	36	39	1337	10	3126	135	6726

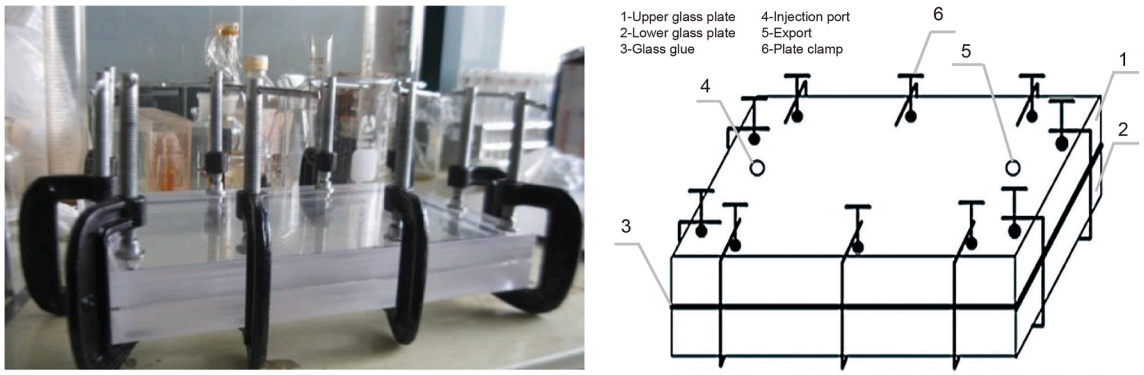

Fig. 1. Picture and schematic diagram of the fracture plate model.

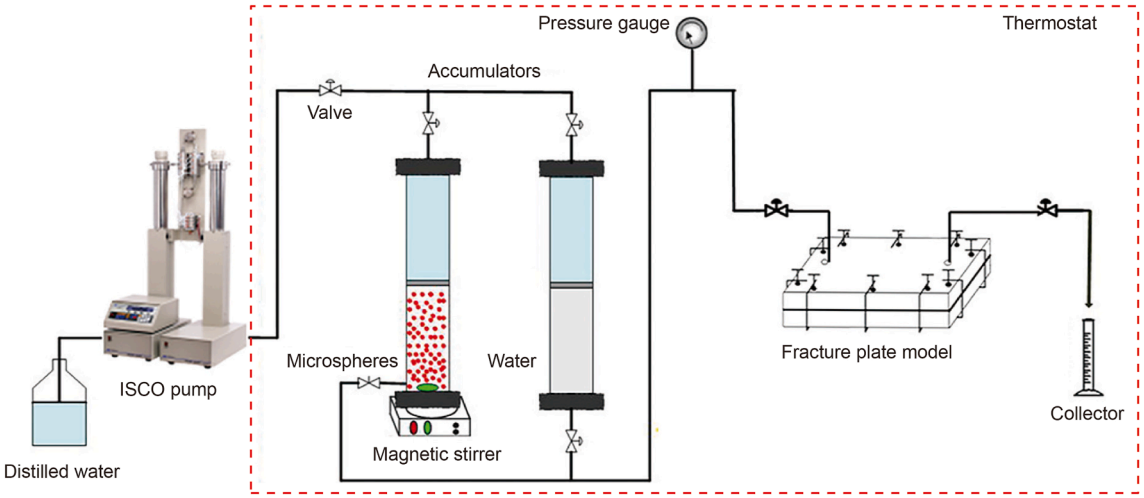

Fig. 2. Flow chart of fracture plate model displacement experiment.

$$S_{rt} / S_{re} = kt^n \quad (2)$$

where S_{rt} is the swelling ratio of low elastic polymer microspheres at time t; S_{re} is the final swelling ratio of low elastic polymer microspheres at swelling equilibrium; k is the swelling rate factor of low elastic polymer microspheres, which represents the characteristics of crosslinking network and solvent system when the microspheres swell; n is the characteristic index of the diffusion mechanism during swelling, which determines the diffusion type during swelling.

Among them, when n is greater than 0.45 and less than 0.5, the diffusion mode of water molecules is Fickian diffusion, the diffusion rate of water molecules into the three-dimensional cross-linked network is much lower than the rate of relaxation and stretching of macromolecular chains in the three-dimensional cross-linked network, and the diffusion of water molecules into the three-dimensional cross-linked network plays a decisive role. When $0.50 < n < 1.0$, it is non-Fickian diffusion, and the diffusion rate of water molecules entering the three-dimensional cross-linked network is equivalent to the relaxation and stretching rate of macromolecules in the three-dimensional cross-linked network segment. When n equals 1, the diffusion mode of water molecules is Case II diffusion. At this time, the diffusion rate of water molecules entering the three-dimensional cross-linked network is much higher than the relaxation and stretching rate of macromolecular chains. The relaxation and stretching of macromolecular chains play a decisive role.

According to Eq. (2), the swelling curve in Fig. 2 is fitted. The fitting results of the swelling curves at the initial stage of swelling ($t < 2$ h) are shown in Fig. 4, and the relevant fitting parameters are shown in Table 3.

It can be seen from Fig. 4 and Table 3 that Fickian equation has a good fitting result for the initial swelling of LEM-1, and the fitting-related parameters are all greater than 0.99. The swelling rate factor at different temperatures is 0.5–1.0, which belongs to non-Fickian diffusion, and the linear fitting degree is good. This indicates that the relaxation rate of macromolecules at the initial stage of swelling is comparable to the diffusion rate of water molecules into the three-dimensional cross-linked network. The swelling rate factor increases with temperature due to accelerated water molecule diffusion and enhanced relaxation of polymer chain segments within the crosslinked network.

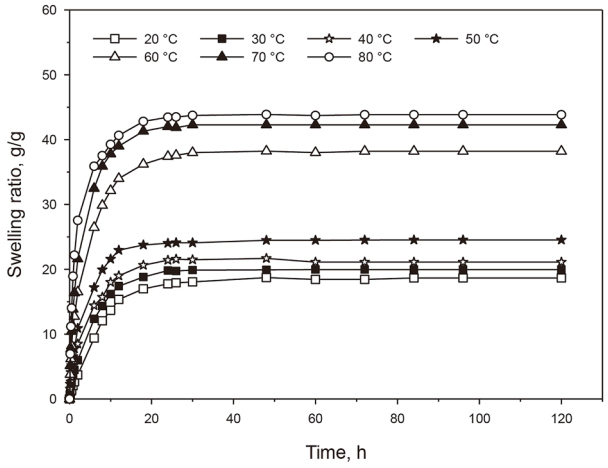

Fig. 3. Swelling curves of LEM-1 microspheres in DG oilfield formation water at different temperatures.

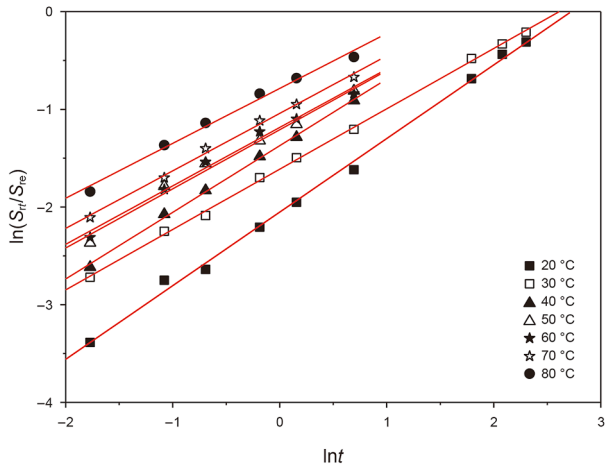

Fig. 4. Fickian curves of swelling kinetics of LEM-1 microspheres at different temperatures.

Table 3
Fitted results of K, n, and R^2 of Fickian curves at different temperatures.

T, °C	K	n	R^2
20	0.128426	0.75332	0.99854
30	0.199349	0.61768	0.99954
40	0.253549	0.68236	0.99912
50	0.298499	0.60530	0.99304
60	0.305538	0.59823	0.99391
70	0.352907	0.58851	0.99777
80	0.455600	0.56208	0.99480

3.1.2. Mid-late swelling process—Schott equation

The Fickian diffusion equation models swelling kinetics as a first-order process, employing idealized approximations where water diffusivity and boundary layer thickness remain constant (Cao B. et al., 2021; Dai et al., 2013). In fact, these two values are constantly changing throughout the process. Since the Fickian equation is only applicable to the initial stage of swelling, it is no longer applicable to the whole swelling process. Therefore, Schott proposed a theoretical model for the whole process and established the following second-order kinetic equation:

$$t/S_{rt} = A + Bt \tag{3}$$

where A and B are constant terms. For the whole swelling process, when the time is relatively long, B is equal to the reciprocal of S_{re}, which is the reciprocal of the equilibrium swelling ratio of the lowelastic polymer microspheres. However, during the initial swelling stage, when t tends to 0, there is $\lim \left(\frac{dS_{rt}}{dt}\right)_{t\to 0} = 1/A$, so A is the reciprocal of the initial swelling rate of low elastic polymer microspheres.

According to Eq. (3), the swelling curve in Fig. 4 is fitted. The fitting results are shown in Fig. 5, and the relevant fitting parameters are shown in Table 4.

From Fig. 5 and Table 4, it can be seen that the Schott equation can be used to fit the whole swelling process of low elastic polymer microspheres. The relevant parameters are all above 0.99, and the fitting degree is good. As the temperature increases, the constants A and B gradually decrease, which indicates that as the temperature increases, the initial swelling rate and the equilibrium swelling ratio of LEM-1 microspheres increase in turn. Elevated temperatures enhance relaxation and swelling kinetics in crosslinked network segments of LEM-1 microspheres, increasing both initial swelling ratios and equilibrium swelling ratios.

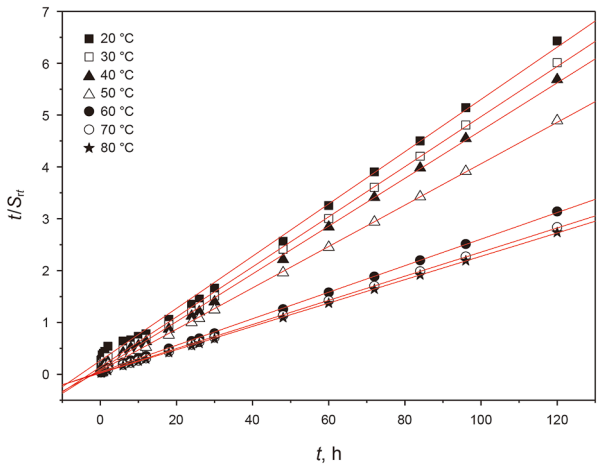

Fig. 5. Schott curves of swelling kinetics of LEM-1 microspheres under different temperatures.

Considering the swelling characteristics of low elastic polymer microspheres, which are fast in the initial stage and gradually slow in the later stage, and combining with the fitting results, the two types of equations are integrated to obtain the swelling kinetic equation of low elastic polymer microspheres:

$$S_{rt} = \begin{cases} 0 & t = 0 \\ kS_{re}t^n & 0 < t < \tau \\ \dfrac{t}{A + Bt} & \tau \le t < t_e \\ S_{re} & t > t_e \end{cases} \tag{4}$$

where τ is the critical swelling time, h. τ is related to the structure of the microsphere itself. For LEM-1, the value is 2.

At a certain temperature and salinity, k, n, A, and B in the swelling kinetic equation (Eq. (4)) can be obtained according to the discrete experimental points. The swelling kinetic equation enables rapid calculation of time-dependent swelling ratios for low-modulus polymer microspheres while quantitatively characterizing their swelling behavior. In addition, according to the kinetic equation, the theoretical chart of the swelling ratio of a low elastic polymer microsphere in different simulated formation water can be drawn, which is convenient for oilfields. Fig. 6 is the theoretical chart of swelling ratio of LEM-1 in DG oilfield formation water.

3.2. Compatibility between polymer microspheres and fractures

The laboratory-made plate model can simulate the width of reservoir fractures by changing the width of the internal gasket (Lin and Sun, 2022). The diameter/width ratio β is defined as the ratio of the diameter of the microsphere to the fracture aperture:

$$\beta = \frac{d_m}{d_f} \tag{5}$$

where β is the diameter/width ratio; d_m is the diameter of polymer microspheres, μm; d_f is the width of the fracture, μm.

Three fracture plate models with different fracture apertures (d_f = 0.1, 0.2, and 0.3 mm) were used. The effects of elastic modulus of microspheres and fracture aperture on the plugging and migration of microspheres in fractures were studied.

3.2.1. Matching of polymer microspheres and reservoir fractures

Fig. 7 shows the injection pressure curves of LEM-1 with elastic modulus of 23.6 Pa when microspheres migrate in the fracture plate model with fracture apertures of 0.1, 0.2, and 0.3 mm, respectively. It can be seen from Fig. 7 that when the swollen LEM-1 microspheres are injected into the fracture plate model with a fracture aperture of 0.3 mm, the injection pressure begins to rise

Table 4
Schott parameters and R^2 of low elastic polymer microspheres (LEM-1) at different temperatures.

T, °C	A	B	R^2
20	0.26256	0.05040	0.99875
30	0.14023	0.04832	0.99953
40	0.09306	0.04608	0.99955
50	0.07021	0.03992	0.99987
60	0.04762	0.02560	0.99987
70	0.03108	0.02326	0.99991
80	0.02234	0.02254	0.99996

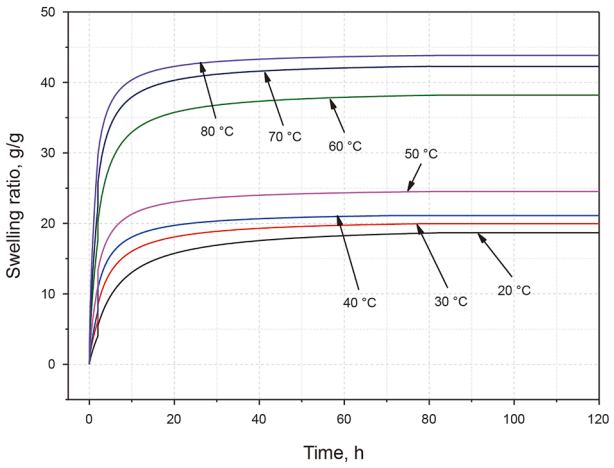

Fig. 6. Theoretical chart for swelling ratio of LEM-1 microspheres in DG oilfield formation water.

first. When the injection volume reaches 7 PV, the injection pressure is basically stable at about 14.3 MPa.

Fig. 8(a) and (d) shows the morphology photos of LEM-1 microspheres before injection and the produced liquid at the outlet end after passing through a 0.3 mm fracture plate model, respectively. It can be found that there is no difference in the particle size of the microspheres in the two images, and the edges are not broken. The average particle size of LEM-1 microspheres after swelling is slightly smaller than the slit width of 0.3 mm, and the diameter/width ratio is about 1. This shows that most of the LEM-1 microspheres can directly pass through the fracture plate model with a fracture aperture of 0.3 mm. When LEM-1 microspheres are injected into the fracture plate model with fracture apertures of 0.2 and 0.1 mm, the injection pressure fluctuates slightly. It can be seen from Fig. 8 that the particle size of LEM-1 microspheres has basically not changed. Since the average particle size of the LEM-1 microspheres after swelling is larger than the fracture aperture (0.2 and 0.1 mm) (the diameter/width ratio is 1.5 and 3.0,

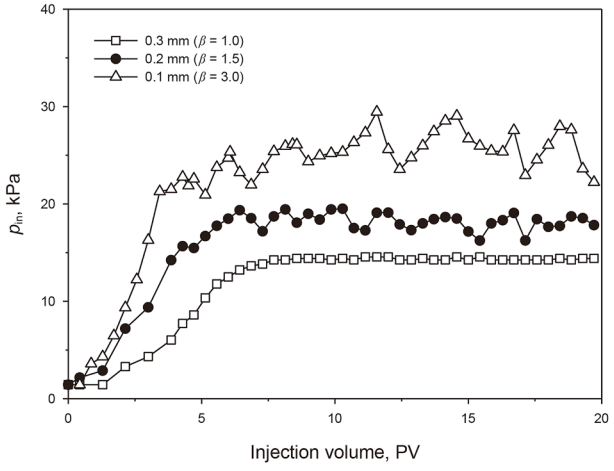

Fig. 7. Injection pressure curves of LEM-1 microspheres under different fracture apertures.

respectively), the swollen LEM-1 microspheres undergo elastic deformation when passing through the fracture plate model with fracture apertures of 0.2 and 0.1 mm, without breaking.

Table 5 summarizes the migration patterns between polymer microspheres with different elastic modulus and plate models with fracture apertures of 0.1, 0.2, and 0.3 mm, respectively. It can be seen from Table 5 that in the experimental range, the migration mode of the microspheres in the fractures is only three cases: straight-through passage, deformable passage, and blockage. The main reason is that the low elastic polymer microspheres will not be easily crushed when the microspheres are injected into the model. Therefore, when the low elastic polymer microspheres are larger than the fracture aperture, only one of them can be selected for deformable passage and blockage. For highly elastic microspheres with elastic modulus greater than 100 Pa, when the microsphere is larger than the fracture aperture, the microsphere will deform through the plate model under the appropriate diameter/width ratio (Tang et al., 2020). However, when the diameter/width ratio is large enough, the compressive deformation ability of the microsphere is not enough to force the microsphere to enter the fracture, the microsphere will block at the injection port. When the injection pressure is large enough, due to the high brittleness of the highly elastic microsphere after swelling, it will be broken at the injection port, and the broken small particles will pass directly through the plate model. In this case, there will be no way for the highly elastic microsphere to break through during the migration of the core pore throat.

3.2.2. Relationship between threshold pressure and elastic modulus of polymer microsphere

To further explore the role of elastic modulus of polymer microspheres during their migration in a fracture plate model, we investigated the relationship between threshold pressure and elastic modulus using a parallel-plate model (Liu et al., 2023; Yang et al., 2019). Threshold pressure refers to the displacement pressure of polymer microspheres when they are first displaced in the model (Yang et al., 2017; Zhao et al., 2023). Fig. 9 shows the relationship between the threshold pressure and the elastic modulus of the microsphere under three different fracture apertures (diameter/width ratio $\beta = 3.0$, 1.5, and 1.0, respectively). It can be seen from the figure that the threshold pressure and elastic modulus are linear under different fracture apertures. The relationship can be expressed as follows:

$$p_t = kG' + m \tag{6}$$

where p_t is the threshold pressure of polymer microsphere migration, Pa; G' is the elastic modulus of polymer microspheres, Pa; k and m are constants, which are related to the diameter/width ratio and the elastic modulus of the microspheres.

It can be seen from Fig. 9 that under the same elastic modulus condition, the smaller the fracture aperture, the higher the threshold pressure. The threshold pressure increased with the increase in elastic modulus under the same fracture aperture. Table 6 lists the fitting equation parameters for the relationship between threshold pressure and elastic modulus. It can be seen that k and m gradually decrease with the increase in fracture aperture. According to Eq. (6), the range of threshold pressure under different fracture apertures can be quantitatively predicted.

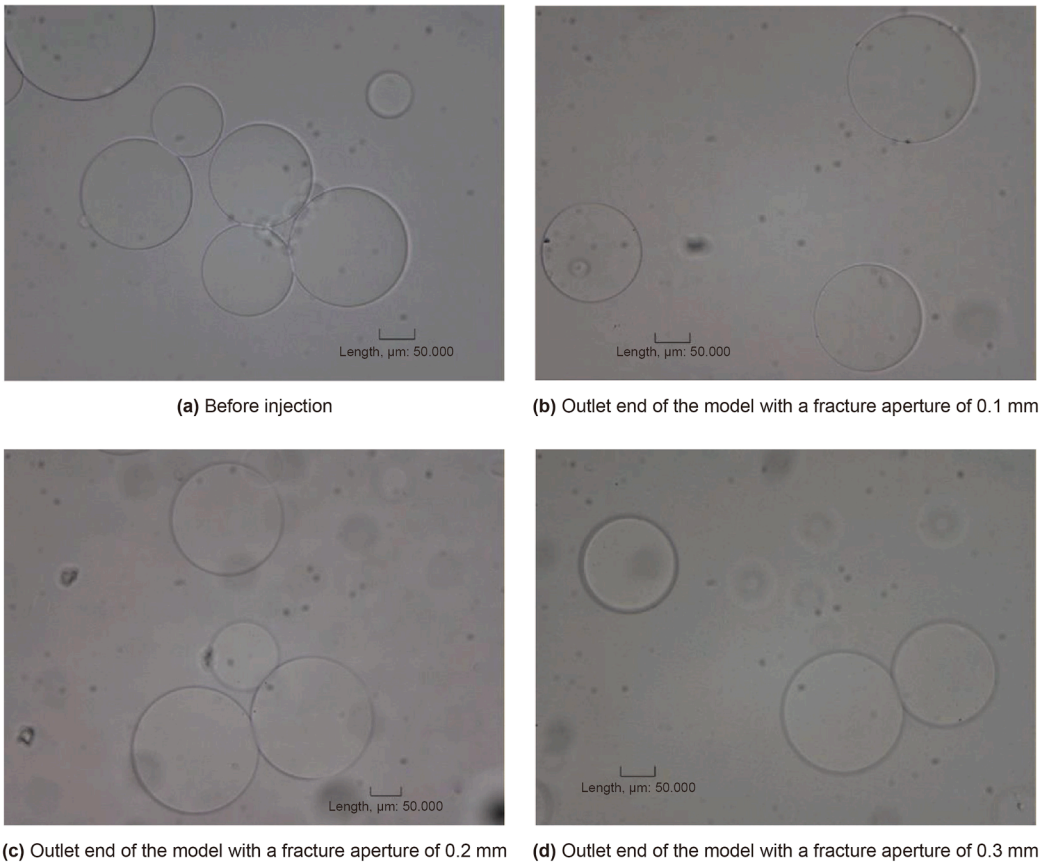

Fig. 8. Morphology photos of LEM-1 microspheres before and after injection in the fracture plate models.

Table 5
Matching relation between polymer microspheres with different elastic modulus and fracture plate model.

Type	Elastic modulus, Pa	Fracture aperture, mm		
		0.3 ($\beta = 1.0$)	0.2 ($\beta = 1.5$)	0.1 ($\beta = 3.0$)
LEM-1	23.6	Straight-through passage	Deformable passage	Deformable passage
LEM-2	32.5	Straight-through passage	Deformable passage	Deformable passage
HEM-1	121	Straight-through passage	Deformable passage	Deformable passage
HEM-2	466	Straight-through passage	Deformable passage	Blockage
HEM-3	715	Straight-through passage	Blockage	Blockage

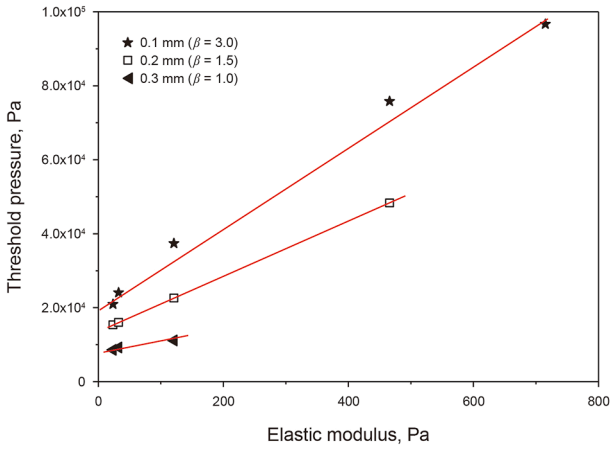

Fig. 9. Relationship curves of threshold pressure and elastic modulus of microspheres under different fracture apertures.

Table 6
Fiting equation parameters for the relationship between threshold pressure and elastic modulus.

Fracture aperture d_f, mm	k	m	R^2
0.1	109.15	21,329.50	0.9916
0.2	74.50	13,609.12	0.9996
0.3	24.26	8231.77	0.9735

4. Conclusions

(1) Taking the swelling ratio as the evaluation index, the swelling kinetics of low elastic polymer microspheres was studied by weighing method. The swelling kinetic equation of low elastic polymer microspheres was proposed, and the swelling ratio theoretical chart of low elastic polymer microspheres (LEM-1) was established.

(2) With the help of the fracture plate model, the compatibility of polymer microspheres and fractures under different

fracture apertures (0.1–0.3 mm) and different elastic modulus (23.6–715 Pa) was systematically studied with the diameter/width ratio as the evaluation index. Equation $p_t = kG' + m$ was established to represent the relationship between the threshold pressure and the elastic modulus of the polymer microspheres as they migrate in the fracture plate model. At different fracture apertures, the threshold pressure of the polymer microspheres is proportional to the elastic modulus of the microspheres.

(3) The physical models used in experiments cannot fully simulate the actual reservoir environment, and there is also a significant discrepancy in the stress field compared to real-field conditions. For future work, it is recommended to develop experimental setups capable of coupling variations in in-situ stress, temperature changes, and chemical flooding processes to more comprehensively evaluate the applicability of microspheres. Additionally, integrating CT scanning technology to construct digital cores and conducting computational fluid dynamics simulations at the pore scale can mutually validate and complement physical experiments, thereby providing deeper insights into the matching mechanism between microspheres and fractures.

CRediT authorship contribution statement

Hong-Bin Yang: Writing – review & editing, Writing – original draft, Resources, Project administration, Funding acquisition. **Lu-Yao Xing:** Writing – review & editing, Writing – original draft, Methodology, Formal analysis, Conceptualization. **Ting-Feng Liu:** Validation, Supervision, Resources, Investigation. **Miao Li:** Validation, Supervision, Project administration, Investigation, Formal analysis. **Jie Geng:** Validation, Supervision, Investigation, Formal analysis. **Yang Zhang:** Visualization, Validation, Supervision, Formal analysis. **Yu-Bin Zhang:** Visualization, Supervision, Software, Data curation, Conceptualization. **Rui-Chao Wang:** Validation, Software, Investigation, Formal analysis. **Bauyrzhan Sarsenbekuly:** Validation, Supervision, Software, Investigation, Formal analysis. **Wan-Li Kang:** Validation, Supervision, Resources, Investigation, Formal analysis, Conceptualization. **Li-Ming Zhang:** Supervision.

Conflict of interest

No conflict of interest exits in the submission of this manuscript, and manuscript is approved by all authors for publication. I would like to declare on behalf of my co-authors that the work described was original research that has not been published previously, and not under consideration for publication elsewhere, in whole or in part. All the authors listed have approved the manuscript that is enclosed.

Acknowledgements

The work was supported by the Fund of Shandong Provincial Natural Science Foundation, China (ZR2025MS783, ZR2024YQ043), the Fundamental Research Funds for the Central Universities (25CX02024A), National Natural Science Foundation of China (52374058), State Key Laboratory of Deep Oil and Gas, China University of Petroleum (East China) (No. SKLDOG2024-ZYRC-06), and Natural Science Basic Research Program of Shaanxi (No. 2023-JC-QN-0486).

References

Barros-Galvis, N., Samaniego, V.F., Cinco-Ley, H., 2018. Fluid dynamics in naturally fractured tectonic reservoirs. J. Pet. Explor. Prod. Technol. 8 (1), 1–16. https://doi.org/10.1007/s13202-017-0320-8.

Budianto, E., Amalia, A., 2020. Swelling behavior and mechanical properties of Chitosan-Poly(N-vinyl-pyrrolidone) hydrogels. J. Polym. Eng. 40 (7), 551–560. https://doi.org/10.1515/polyeng-2019-0169.

Cao, B., Xie, K., Lu, X.G., et al., 2021. Effect and mechanism of combined operation of profile modification and water shutoff with in-depth displacement in high-heterogeneity oil reservoirs. Colloids Surf. A Physicochem. Eng. Asp. 631. https://doi.org/10.1016/j.colsurfa.2021.127673.

Cao, M.J., Cai, Q., Guo, G.F., et al., 2021. The preparation and displacement performances of a hollow structure microsphere with swelling–deswelling properties for enhanced oil recovery (EOR). Polym. Bull. 79 (6), 4323–4337. https://doi.org/10.1007/s00289-021-03712-y.

Chen, X., Li, Y.Q., Liu, Z.Y., et al., 2020. Core- and pore-scale investigation on the migration and plugging of polymer microspheres in a heterogeneous porous media. J. Petrol. Sci. Eng. 195. https://doi.org/10.1016/j.petrol.2020.107636.

Cheng, L., Xie, Y., Chen, J., et al., 2024. Multi-scale visualization study of water and polymer microsphere flooding through horizontal Wells in low-permeability oil reservoir. Energies 17 (18). https://doi.org/10.3390/en17184597.

Dai, B.M., Xu, P., Xu, M.B., et al., 2023. Synthesis and plugging effect of inverse emulsion polymerization microspheres (OPME) for oil-based drilling fluids. Arab. J. Chem. 16 (4). https://doi.org/10.1016/j.arabjc.2023.104577.

Dai, C.L., Zhao, J., Jiang, H.Q., et al., 2013. Research and field application of polymer-multiple emulsion crosslinker gel for the deep profile control. Petrol. Sci. Technol. 31 (9), 902–912. https://doi.org/10.1080/10916466.2010.531340.

Diwu, P., Jiang, B., Hou, J., et al., 2018. Experimental study on expansion characteristics of core-shell and polymeric microspheres. J. Nanotechnol. 2018 (1). https://doi.org/10.1155/2018/7602982.

Du, D.J., Pu, W.F., Zhang, S., et al., 2020. Preparation and migration study of graphene oxide-grafted polymeric microspheres: EOR implications. J. Petrol. Sci. Eng. 192. https://doi.org/10.1016/j.petrol.2020.107286.

Hou, G.G., Zhao, W.Y., Jia, Y.Q., et al., 2020. Field application of nanoscale polymer microspheres for in-depth profile control in the ultralow permeability oil reservoir. Front. Chem. 8. https://doi.org/10.3389/fchem.2020.00805.

Hua, Z., Lin, M.Q., Dong, Z.X., et al., 2014. Study of deep profile control and oil displacement technologies with nanoscale polymer microspheres. J. Colloid Interface Sci. 424, 67–74. https://doi.org/10.1016/j.jcis.2014.03.019.

Jiang, H.Z., Yang, H.B., Pan, R.S., et al., 2024. Performance and enhanced oil recovery efficiency of an acid-resistant polymer microspheres of anti-CO_2 channeling in low-permeability reservoirs. Pet. Sci. 21 (4), 2420–2432. https://doi.org/10.1016/j.petsci.2024.02.002.

Jiang, H.Z., Yang, H.B., Ning, C.Y., et al., 2025. Amphiphilic polymer with ultra-high salt resistance and emulsification for enhanced oil recovery in heavy oil cold recovery production. Geoenergy Sci. Eng. 252, 213920. https://doi.org/10.1016/j.geoen.2025.213920.

Jie, C., Hu, M.M., Cheng, Y., et al., 2024. Design of degradable hybrid dual-crosslinked polymer for high-efficiency profile control in high temperature reservoirs. Colloids Surf. A Physicochem. Eng. Asp. 698. https://doi.org/10.1016/j.colsurfa.2024.134530.

Li, J.B., Niu, L.W., Lu, X.G., 2019. Migration characteristics and deep profile control mechanism of polymer microspheres in porous media. Energy Sci. Eng. 585. https://doi.org/10.1002/ese3.409.

Li, J.B., Niu, L.W., Wu, W.X., et al., 2020. The reservoir adaptability and oil displacement mechanism of polymer microspheres. Polymers 7 (5), 16–2045. https://doi.org/10.3390/polym12040885.

Li, Y.I., Zhou, M., Huang, J.X., et al., 2024. Preparation of polymer microspheres as oil displacement agent for extra-high temperature and extra-high salinity reservoirs. Colloids Surf. A Physicochem. Eng. Asp. 685. https://doi.org/10.1016/j.colsurfa.2024.133303.

Lin, R.Y., Sun, L., 2022. Numerical simulation of the microscopic plugging mechanism and particle flow process of the microsphere system. ACS Omega 7 (50), 46983–46991. https://doi.org/10.1021/acsomega.2c06088.

Liu, K.C., Wang, R., Rong, K.S., et al., 2023. Synthesis and plugging performance of nano-micron polymeric gel microsphere plugging agents for oil-based drilling fluids. Gels 9 (4). https://doi.org/10.3390/gels9040290.

Liu, W.J., Li, J., Luo, T.T., et al., 2024. Research on crack sealing performance of polymer microsphere/hydrogel composite system. Processes 12 (11). https://doi.org/10.3390/pr12112483.

Liu, Y.F., Yang, J.W., Wu, T.J., et al., 2020. Pore-scale investigation on the plugging behavior of submicron-sized microspheres for heterogeneous porous media with higher permeability. Geofluids. https://doi.org/10.1155/2020/8869760.

Lu, S.Y., Bo, Q.W., Zhao, G., et al., 2023. Recent advances in enhanced polymer gels for profile control and water shutoff: A review. Front. Chem. 11. https://doi.org/10.3389/fchem.2023.1067094.

Shagymgereyeva, S., Sarsenbekuly, B., Kang, W.L., et al., 2023. Advances of polymer microspheres and its applications for enhanced oil recovery. Colloids Surf. B Biointerfaces 233. https://doi.org/10.1016/j.colsurfb.2023.113622.

Song, Z.Z., Hu, J.H., Liu, P., et al., 2023. Synthesis and performance evaluation of alginate-coated temperature-sensitive polymer gel microspheres. Gels 9 (6). https://doi.org/10.3390/gels9060480.

Tang, X.C., Kang, W.L., Zhou, B.B., et al., 2020. Characteristics of composite microspheres for in-depth profile control in oilfields and the effects of polymerizable silica nanoparticles. Powder Technol. 359, 205–215. https://doi.org/10.1016/j.powtec.2019.09.070.

Tao, S.Y., Ding, Y.Z., Jiang, L., et al., 2016. Preparation of magnetic hierarchically porous microspheres with temperature-controlled wettability for removal of oils. J. Colloid Interface Sci. 492, 73–80. https://doi.org/10.1016/j.jcis.2016.12.069.

Wang, J.Q., Kang, W.L., Yang, H.B., et al., 2022. Study on salt tolerance mechanism of hydrophobic polymer microspheres for high salinity reservoir. J. Mol. Liq. 368. https://doi.org/10.1016/j.molliq.2022.120639.

Wang, J., Zhou, F.J., Li, J.J., et al., 2019. Evaluation of the oil/water selective plugging performance of nano-polymer microspheres in fractured carbonate reservoirs. J. Zhejiang Univ. - Sci. A 20 (9), 714–726. https://doi.org/10.1631/jzus.A1900249.

Wang, L., Liang, J.Y., He, L., 2014. Superhydrophobic and oleophobic surface from fluoropolymer–SiO_2 hybrid nanocomposites. J. Colloid Interface Sci. 435, 75–82. https://doi.org/10.1016/j.jcis.2014.08.017.

Wu, Q.H., Ge, J.J., Ding, L., et al., 2021. Insights into the key aspects influencing the rheological properties of polymer gel for water shutoff in fractured reservoirs. Colloids Surf. A Physicochem. Eng. Asp. 634. https://doi.org/10.1016/j.colsurfa.2021.127963.

Yan, C.L., Zhang, P.H., Dong, L.F., et al., 2024. Long-term fracture conductivity in tight reservoirs. Energy Sci. Eng. 12 (3), 1187–1199. https://doi.org/10.1002/ese3.1708.

Yang, H.B., Kang, W.L., Yin, X., et al., 2017. Research on matching mechanism between polymer microspheres with different storage modulus and pore throats in the reservoir. Powder Technol. 313, 191–200. https://doi.org/10.1016/j.powtec.2017.03.023.

Yang, H.B., Kang, W.L., Tang, X.C., et al., 2018. Gel kinetic characteristics and creep behavior of polymer microspheres based on bulk gel. J. Dispersion Sci. Technol. 39 (12), 1808–1819. https://doi.org/10.1080/01932691.2018.1462192.

Yang, H.B., Shao, S., Zhu, T.Y., et al., 2019. Shear resistance performance of low elastic polymer microspheres used for conformance control treatment. J. Ind. Eng. Chem. 79, 295–306. https://doi.org/10.1016/j.jiec.2019.07.005.

Yang, H.B., Zhou, B.B., Zhu, T.Y., et al., 2020. Conformance control mechanism of low elastic polymer microspheres in porous medium. J. Petrol. Sci. Eng. 196. https://doi.org/10.1016/j.petrol.2020.107708.

Yang, H.B., Jiang, H.Z., Xu, Z., et al., 2025a. Development and evaluation of organic/metal ion double crosslinking polymer gel for anti-CO_2 gas channeling in high temperature and low permeability reservoirs. Pet. Sci. 22, 725–738. https://doi.org/10.1016/j.petsci.2024.11.016.

Yang, H.B., Li, H.C., Jiang, H.Z., et al., 2025b. Effect of surface hydrophobicity of fluorescent nanopolymer microspheres on the stability of CO_2 foam. Langmuir 41 (20), 12704–12717. https://doi.org/10.1021/acs.langmuir.5c00878.

Yang, H.B., Jiang, H.Z., Liu, T.F., et al., 2025c. Viscoelastic displacement mechanism of fluorescent polymer microspheres based on macroscopic and microscopic displacement experiments. Phys. Fluids 37 (4). https://doi.org/10.1063/5.0268850.

Yang, H.B., Li, H.C., Xu, H., Wang, R.C., et al., 2026. Enhanced CO_2 foam stabilization with fluorescent nano polymer microspheres for improved oil recovery: Insights from microscopic and macroscopic displacement studies. Geoenergy Sci. Eng. 257. https://doi.org/10.1016/j.geoen.2025.214222.

Yang, H.D., Zhang, D.X., Wang, Y., et al., 2024. Experimental study of synergy between polymeric microspheres and nanoemulsions for profile control and water plugging. ACS Omega 9 (43), 43756–43765. https://doi.org/10.1021/acsomega.4c06346.

Zhao, F.J., Zhang, H.B., Wu, Y.P., et al., 2020. Preparation and performance evaluation of polymeric microspheres used for profile control of low-permeability reservoirs. J. Chem. 2020. https://doi.org/10.1155/2020/5279608.

Zhao, S., Pu, W.F., 2020. Migration and plugging of polymer microspheres (PMs) in porous media for enhanced oil recovery: Experimental studies and empirical correlations. Colloids Surf. A Physicochem. Eng. Asp. 597. https://doi.org/10.1016/j.colsurfa.2020.

Zhao, T.H., Xing, J.Y., Pu, W.F., et al., 2016. Synthesis and property evaluation of a novel polyacrylamide-montmorillonite composite for water shutoff and profile control in high salinity reservoirs. Polym. Compos. 39 (2), 368–376. https://doi.org/10.1002/pc.23945.

Zhao, Z., Sun, J.S., Liu, F., et al., 2023. Micro-nano polymer microspheres as a plugging agent in oil-based drilling fluid. Colloids Surf. A Physicochem. Eng. Asp. 673. https://doi.org/10.1016/j.colsurfa.2023.131808.

Zhong, H.Y., Shen, G.C., Qiu, Z.S., et al., 2018. Minimizing the HTHP filtration loss of oil-based drilling fluid with swellable polymer microspheres. J. Petrol. Sci. Eng. 172, 411–424. https://doi.org/10.1016/j.petrol.2018.09.074.